



Bioinspired multifunctional self-powered ionic receptors derived by gradient polyelectrolyte hydrogels

Xiaobin Zhu, Pengfei Qi ^{*}, Wenxin Fan ^{*}, Haojie Wang, Kunyan Sui ^{*}

State Key Laboratory of Bio-Fiber and Eco-textiles, College of Materials Science and Engineering, Collaborative Innovation Center for Marine Biobased Fibers and Ecological textile technology, Institute of Marine Biobased Materials, Qingdao University, Qingdao 266071, PR China



ARTICLE INFO

Keywords:
Bionic ionic sensors
Gradient hydrogels
Self-induced potential
Self-powered devices
Multiple sensing abilities

ABSTRACT

Emerging ionic diode-based self-powered ionic devices are intriguing in mimicking human perceptual systems. However, challenges remain for their applications such as undesired delamination between diode components, single function of press perception, and limited stretchability and transparency caused by metal/carbonous electrodes. Herein, we demonstrate a versatile strategy for constructing multifunctional self-powered ionic receptors/sensors. The gradient polyelectrolyte hydrogel has been firstly demonstrated to hold a pressure-sensitive built-in potential analogous to ionic diodes, but can avoid their defect of delamination. The receptor is assembled by two stretchable ionic hydrogel electrodes and a sandwiched gradient polyelectrolyte hydrogel, resembling the structure of electrolyte/cell membrane/electrolyte of human receptors. Benefiting from such sandwich structure, the as-prepared self-powered receptors are highly transparent, stretchable, and multifunctional. They not only can sensitively perceive tiny pressure change based on the thickness-dependent potentials of gradient hydrogels, but temperature, salinity and pH stimuli according to the potential variations induced by thermodiffusion and salinity gradient. The strategy can inspire the design and fabrication of high-performance self-powered sensors consisting entirely of ionic conductors, contributing to the development of complex humanlike sensing systems in the future.

1. Introduction

As one of the essential components of reflex arcs, the widespread receptors play key roles in communicating with the surrounding environment for human bodies.^[1–3] For example, the receptors in human skins and tongues can perceive the external mechanical and chemical stimuli via the potential variations of cell membranes, which are then transported to the brain by nerves to form sensory feedback.^[4–6] Specifically, when the sensory cells are in a resting state, the cell membranes stay in a polarized state, exhibiting a lower potential inside the cells (Fig. 1a). The external stimuli can open the mechanically/chemically gated ion channels to induce the influx of sodium ions into cells, leading to an obvious rise of membrane potential (also known as the depolarization process).^[4–6] After removing external stimuli, the membrane potential returns to the initial level by driving specific ions back across the cell membranes (repolarization process).

In order to recreate the properties of human sensory systems in various stretchable wearable devices, great efforts have been devoted to designing various artificial electronic/ionic sensors with high

sensitivity,^[7–9] low detection limit,^[11–12] multi-sensing capacity,^[13–16] and self-healing capability.^[17–19] Among others, the stretchable self-powered sensors have drawn great attentions, since they can transform the external stimuli into potential signals like human sensory systems as well as circumvent the heavy and bulky power supply units.^[20–25] However, the conventional self-powering sensors based on stretchable triboelectric and piezoelectric nanogenerators transport signals via electrons, differing with signal carriers (i.e., ions) of human sensory systems.^[26–35] Meanwhile, these self-powered electronic sensors generally displayed the inefficient power density at low frequencies and low charge amounts, because the potential distribution and charges are only created on the surface of piezoelectric and triboelectric materials.^[7,10,36] In this regard, the ionic diodes that consist of a pair of polycation and polyanion conductors have shown great potential as self-powered ionic sensors.^[37–40] They can provide much longer current duration and higher power density under low-frequency mechanical stimuli, as the whole ionic diodes are involved in the charge generation.^[37–40] Nevertheless, such ionic diode-based devices could suffer from unwanted delamination between diode components, and

^{*} Corresponding author.

E-mail addresses: pengfei@uni-bremen.de (P. Qi), fanwenxin@qdu.edu.cn (W. Fan), sky@qdu.edu.cn (K. Sui).

limited stretchability and transparency due to the applied metal/carbonous electrodes. Additionally, the ionic diode-based sensors merely respond to mechanical stimuli and cannot perceive the thermal and chemical stimuli highly associated with human physiological activities. Therefore, it remains a great challenge to design and fabricate stretchable and multifunctional self-powered ion-based sensors/receptors capable of replicating diverse functions of human sensory systems.

Herein, we present a general strategy towards constructing bionic multifunctional self-powered ionic sensors/receptors. The gradient polyelectrolyte hydrogels have been firstly exploited as ion-based mechanoelectric conversion materials, possessing pressure-sensitivity self-induced potential similar to reported ionic diodes, but avoiding the delamination between diode components (Fig. 1b). Different from the ionic diode-based sensors that rely on un-stretchable metallic electrodes, the self-powered receptor is integrated readily by sandwiching a gradient polyelectrolyte hydrogel sheet between two stretchable ionic hydrogel-based electrodes. Such a structure resembles that of human sensory receptors, in which the gradient polyelectrolyte hydrogel and the two ionic hydrogels function as the polarized sensory cell membrane and extracellular/intracellular electrolytes, respectively (Fig. 1c). Notably, the sandwich structure enables the self-powered ionic receptor to have high transparency, high stretchability and multiple perception abilities. Besides of the high-resolution pressure-perception function based on the thickness-dependent potential of gradient hydrogel, the ionic receptors can also precisely perceive thermal and chemical stimuli via the potential variations induced by the thermodiffusion and salinity gradient. The strategy can inspire the design and fabrication of self-powered all-ion-based sensors, contributing to the development of complex humanlike sensing systems in the future.

2. Experimental section

2.1. Materials

Acrylamide (AM, > 98%), and glycidyl methacrylate (GMA, 97%), N,N'-methylenebisacrylamide (BIS, 98%), and N,N,N',N'-

tetramethylethylenediamine (TEMED, 99%) were purchased from Aladdin Reagents Co. (Shanghai, China). Ammonium peroxodisulfate (APS, 99.99%), KOH (95%), NaCl, NaOH, HCl, CH₃COOH, and ethanol were supplied by Hydroquinone Sinopharm Chemical Reagent, China. Chitosan (CS, *Mw* = 700000) with a deacetylation degree of ≥ 90.0% was purchased from Blue season biology Co., Ltd. (Shanghai, China). Sodium alginate (SA, G/M = 2:1, *Mw* = 380000) was provided by Qingdao Hyzlin Biology Development Co., Ltd. (Shandong, China).

2.2. Modification of chitosan

Firstly, a previous solution containing 3 g CS, 2.4 g acetic acid and 97.6 g deionized water was added into a three-necked flask. After the chitosan dissolving, 5 mL of 5 M/L KOH solution, 10 mL hydroquinone solution and 0.1 mL GMA was subsequently added into the above solution dropwise. The solution was circulated in nitrogen for 30 min, and then heated to 65 °C under stirring for 2 h. The mixed solution was washed and filtered with ethanol solution for three times, and the final methacrylated CS (MCS) was obtained after freeze-drying.

2.3. Modification of SA

2 wt% SA solution respect to the weight of deionized water was firstly prepared. 0.4 mL GMA was then added into the above solution and stirred for 4 h at 60 °C in dark conditions. The pH of the solutions was adjusted and kept around 3 during the whole reaction processes. The obtained solution was washed and filtered using ethanol solution for three times, and then washed with deionized water. The final methacrylated SA (MSA) was obtained after freeze-drying.

2.4. Preparation of the gradient polyelectrolyte hydrogels

The gradient PAM/MCS hydrogels were fabricated by electric field-assisted free radical polymerization (Figure S1a). In brief, 5.33 g AM (monomer), 3.19 mg MBAA (cross-linker), 5.33 mg APS (initiator) and 21 μL TEMED (catalyst) were sequentially dissolved into 30 mL MCS

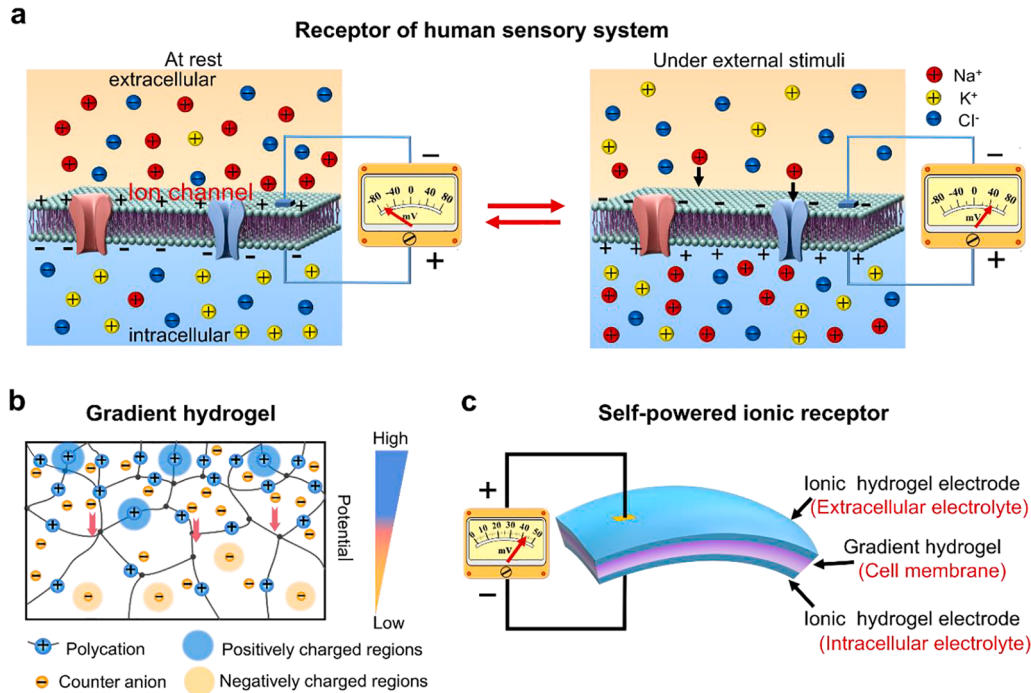


Fig. 1. Principles for the design of self-powered ionic receptor. (a) Diagram depicting the variation of membrane potential during the applying and removing of a stimulus. (b) Mechanism diagram of gradient polyelectrolyte hydrogels with self-induced potential. (c) Schematic diagram of the receptor comprising of stretchable ionic hydrogel electrodes and a sandwiched gradient polyelectrolyte hydrogel.

solution with different concentrations under stirring in an ice bath. After centrifugation and defoaming, the precursor solution was injected into a home-made mold consisting of two ITO conductive glasses and a spacer. Subsequently, a 1.5 V direct-current (DC) voltage was applied on the mold and kept at room temperature for one hour to promote the migration of MCS toward the cathode. Then, the mold in a power-on state was placed into a 50 °C oven for half an hour, and the hydrogel continue to react for another two and a half hours after a power outage. A gradient hydrogel was finally obtained during the coupling processes of electric field-induced diffusion of charged MCS and thermal-initiated polymerization. The gradient PAM/MSA hydrogel sheet was prepared by the similar method.

2.5. Preparation of the receptors

The receptors were prepared by directly synthesizing PAM/NaCl hydrogels on both the top and bottom surface of gradient polyelectrolyte hydrogels (Figure S1b). A precursor solution containing 19.9 wt% AM, 0.45 wt% NaCl, MBAA, APS and TEMED was firstly prepared in an ice bath. The solution was then injected into the molds and in-situ polymerized at both the upper and lower surfaces of the gradient hydrogel. Similar preparation steps were also applicable for another types of receptors prepared using PAA/NaCl ionic hydrogels.

2.6. Characterization

Chemical structure information of the MCS and MSA were characterized by Fourier transform infrared spectroscopy (FTIR, Nicolet-is 50) and Nuclear magnetic resonance spectroscopy (NMR, Bruker AVANCE, Germany), respectively. The cross-sectional morphologies of the gradient PAM/MCS hydrogels were observed using scanning electron microscope (SEM, Quanta 250 FEG). The gradient distribution (charge distribution) of the hydrogel was also analyzed by confocal laser scanning microscope (CLSM, Axio-Imager LSM-800). Before testing, the hydrogel was dyed by the diluted solution of negatively charged sodium fluoresce (10⁻² M). The element content distribution on the upper and lower surfaces of the gradient hydrogels were analyzed using X-ray photoelectron spectroscopy (XPS, Thermo Scientific Escalab 250Xi +). The transparency of the receptors was characterized by Ultraviolet and visible spectrophotometer (UV-vis, T9). The mechanical properties of the receptors were tested by universal testing machine (WD-5 T, China). The sensing performance and the output voltage of the receptors regarding external stimulus such as pressure, strain, temperature, saline solution, acid and base solution, were monitored by a digital source meter (Keithley 2450, USA). Infrared thermographic camera (Xi400, Optis) was also used to conduct thermal imaging tests for evaluating thermal sensing performance of the receptors.

3. Results and discussion

3.1. Preparation and characterization

The gradient polyelectrolyte hydrogels were prepared by electric field-assisted free radical polymerization in the home-made molds consisting of two conductive glasses and a spacer (Figure S1a). The precursor solution consisted of acrylamide (AM, monomer), methacrylated chitosan (MCS, polycation), N,N'-methylene-bis-acrylamide (MBA, cross-linking agent), ammonium peroxodisulfate (APS, initiator), and N,N,N',N'-tetramethylethylenediamine (TEMED, accelerator). The MCS was firstly prepared by modifying CS with glycidyl methacrylate (Figure S2, see more detailed description in Note S1). [41] The MCS polycations moved directionally toward the cathodes under the drive of 1.5 V DC voltage. And meanwhile, the MCS crosslinked with AM by double bonds during heat-polymerization processes to solidate the gradient structure. Therefore, the resulting polyacrylamide (PAM)/MCS hydrogels possesses a higher chain density of MCS and hence a higher

positively charged group density at cathode side (denoted as HD side) than that at anode side (denoted as LD side), as shown in Fig. 2a. The gradient distribution of positively charged groups can be visually validated by the characterization of confocal laser scanning microscopy (CLSM). Clearly, the negatively charged sodium fluorescein demonstrates a gradient distribution within the hydrogel (Fig. 2b). Besides, compared with the LD side, the HD side of the PAM/MCS hydrogel exhibits a lower nitrogen content, further demonstrating the higher chain density of MCS on this side (Fig. 2c). Because the MCS was copolymerized onto the PAM networks by bound bonds (Figure S3), the gradient structures of hydrogel can be solidified permanently, as reflected by the cross-sectional SEM images and stable self-induced potential of gradient hydrogels after storage in the air for one month (Figure S4).

The ionic receptor was then prepared by directly synthesizing two PAM/NaCl hydrogel electrodes on top and bottom surfaces of the gradient PAM/MCS hydrogel (Figure S1b). The ionic receptors are highly transparent and stretchable (Fig. 2d). For example, the SPI-receptor prepared with 2 wt% MCS can present a transmittance of 93% in the visible light wavelength range of 400–800 nm and a large breaking strain of 634% (Fig. 2e and f). Notably, the high MCS content is detrimental to the mechanical properties of SPI-receptors, due to the excessively high crosslinking density induced by the copolymerization of the vinyl groups on MCS and AM monomer. [42] There exists a built-in potential on the gradient polyelectrolyte hydrogel due to the spontaneous diffusion of counter ions under concentration gradient (Fig. 1b). [43–45] The self-induced potential or open-circuit voltage of self-powered receptor is determined by that of gradient hydrogel whose potential value increases with the increasing content of MCS (Fig. 2g).

3.2. Pressure- and strain-sensing performance

The maximum output voltage of the receptor decreased as the application of a compressive force (Fig. 3a). Here, the pressure sensitivity (S_p) of the receptors is evaluated by $S_p = |\Delta V / \Delta P|$, where ΔV and ΔP are the variations of output voltage and applied pressure. Notably, in order to maintain a steady ion/electron interface during the test, the external mechanical stimuli were intentionally applied on the positions far away from the metal electrodes (Figure S5). As the receptors prepared with 2 wt% MCS have a higher sensitivity than the receptors fabricated with other concentrations, they were used in the following tests (Fig. 3a and S6a). The pressure sensitivity of the receptor for this case is calculated to be 116.13 mV/MPa at a small pressure lower than 0.21 MPa, and decreases to 4.57 mV/MPa as the strain increases over 0.66 MPa. Besides, we have systematically studied the effect of DC voltage and device size on the pressure sensitivity of SPI-receptors (Figure S7). The device size shows a little influence on the sensing sensitivity of SPI-receptors, while their pressure sensitivity increases with the increasing of the applied DC voltage used for preparing the gradient polyelectrolyte hydrogels. In this work, the 1.5 V DC voltage was utilized because a higher voltage would cause the serious electrolysis of water and the severe etching of the surface of gradient polyelectrolyte hydrogels.

When a constant pressure was applied on the receptor, its output voltage reduced to a stable value with subtle fluctuations. The fluctuation range of the output voltage was as low as 0.04%. Once the pressure was removed, the output voltage returned to its initial value (Fig. 3b). The response and recovery time of SPI-receptors are 0.36 s and 0.48 s, respectively. It suggests that the receptors are capable of detecting low-frequency/static mechanical stimuli. They can response to a very small pressure of 0.05 kPa, and produce reproducible waveforms under repeated loading/unloading processes in a wide pressure range (0.05–2.50 kPa). When a static pressure (12.5 kPa) is applied on the receptor persistently, its output voltage can be kept at a constant lower value (Fig. 3c). Besides, the SPI-receptors show outstanding long-term stability, and can maintain a stable relative voltage change ratio

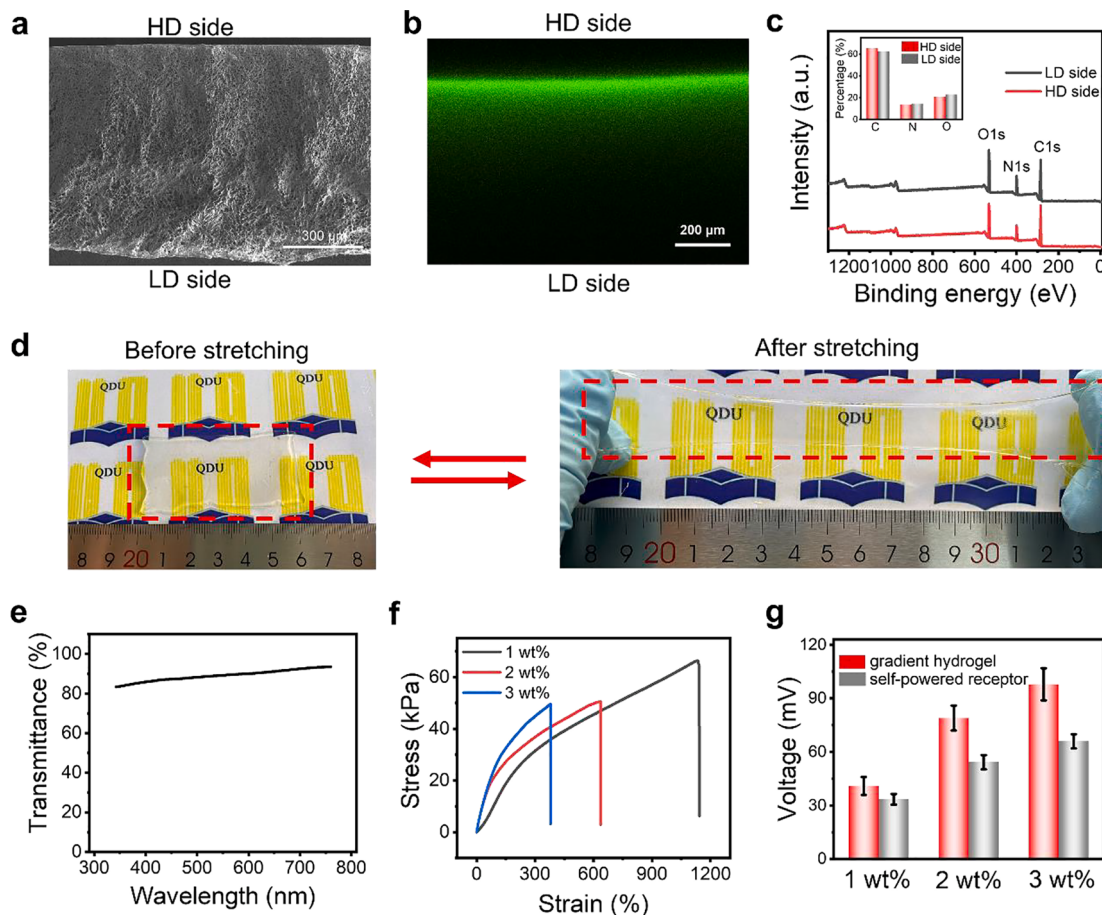


Fig. 2. Characterization of the self-powered ionic receptors. (a) Cross-sectional SEM images of gradient PAM/MCS hydrogel. (b) CLSM image of gradient PAM/MCS hydrogel, and the negatively charged sodium fluorescein (green fluorescence) demonstrate a gradient distribution within the hydrogel. (c) Wide-scan survey XPS spectra of the HD side and LD side for gradient PAM/MCS hydrogel, and the insert is the atomic percentage of carbon, nitrogen and oxygen at the HD side and LD side. (d) The optical images of receptors before and after stretching. (e) Transmittance spectra of the self-powered ionic receptor. (f) Stress-strain curves of the receptors with different MCS contents. (g) Self-induced potential of gradient PAM/MCS hydrogels and corresponding receptors with different MCS contents.

after >10,000 cycles at a pressure of 1.25 kPa (Fig. 3d). Moreover, we have explored the mechanoelectric conversion ability of SPI-receptors. As shown in Figure S8a, the as-prepared SPI-receptors presented a high power density of 0.206 $\mu\text{W cm}^{-2}$, superior to that of triboelectric and piezoelectric energy harvester.[46] Besides, the SPI-receptors also hold a longer current duration time with a full width at half maximum (FWHM) of 6.8 s (Figure S8b), while the FWHM of triboelectric and piezoelectric energy harvester is ~100 ms.[47,48]

The receptors also can be utilized to detect the strain change. Its maximum output voltage was decreased when being stretched (Fig. 3e). The strain sensitivity (S_e) is defined as $S_e = |\Delta V / \Delta \epsilon|$, where $\Delta \epsilon$ is the change of the applied strain. A relatively high strain sensitivity of 2.72 can be obtained at a small strain lower than 40%, and decreases to 1.40 as the strain increases to 120%. When applying a constant strain (300%), the output voltage of receptor decreases to a constant value and returns to the initial value after removing the strain (Figure S6b). The receptor possesses a wide strain sensing range (>120%), and can generate the reproducible waveforms in response to the strains ranging from 1% to 120% (Fig. 3f). They also present outstanding durability and long-term stability in response to tensile strains. Under repeated loading and unloading of 60% strain, the receptor still can present stable electrical responses before and after storage in the atmosphere for one month (Figure S9). The SPI-receptor presented a large detect range and an ultralow detection limit, which are comparable to the state-of-the-art sensors constructed based on homogeneous hydrogels (Figure S10).

Based on the outstanding pressure- and strain-sensing performance,

the receptors can act as self-powered ionic skins to monitor diverse human motions. As a result of the large strain detection range, they can track the bending motions of the joints of finger, wrist, knee, and elbow in real time regardless of their bending speed (Fig. 3g, h, and Figure S11). For instance, when mounted over a finger, a stepwise decrease of output voltage can be observed as the bending angle of finger increases step by step. Meanwhile, the high pressure resolution enables the receptor to accurately record subtle motions of pulse (Fig. 3i), in which three distinctive diacritical peaks in each circulation could carry important disease-associated information of human cardiovascular systems.[49,50]

3.3. Mechanoelectric conversion mechanism of gradient polyelectrolyte hydrogel

To reveal the pressure- and strain-sensing mechanism of the receptors, we have quantitatively analyzed the self-induced built-in potential of gradient PAM/MCS hydrogel, since it determines the potential of the receptor. Here, the self-induced potential ($\Delta\phi$) of gradient hydrogel can be represented as follows (see detailed description in Note S2):

$$\Delta\phi = \frac{RT}{F} \ln \frac{c_{Ac} - (h)}{c_{Ac} - (l)} \quad (1)$$

where F , R and T are the Faraday constant, gas constant, and temperature, respectively, $c_{Ac}(h)$ and $c_{Ac}(l)$ are the concentrations of counter

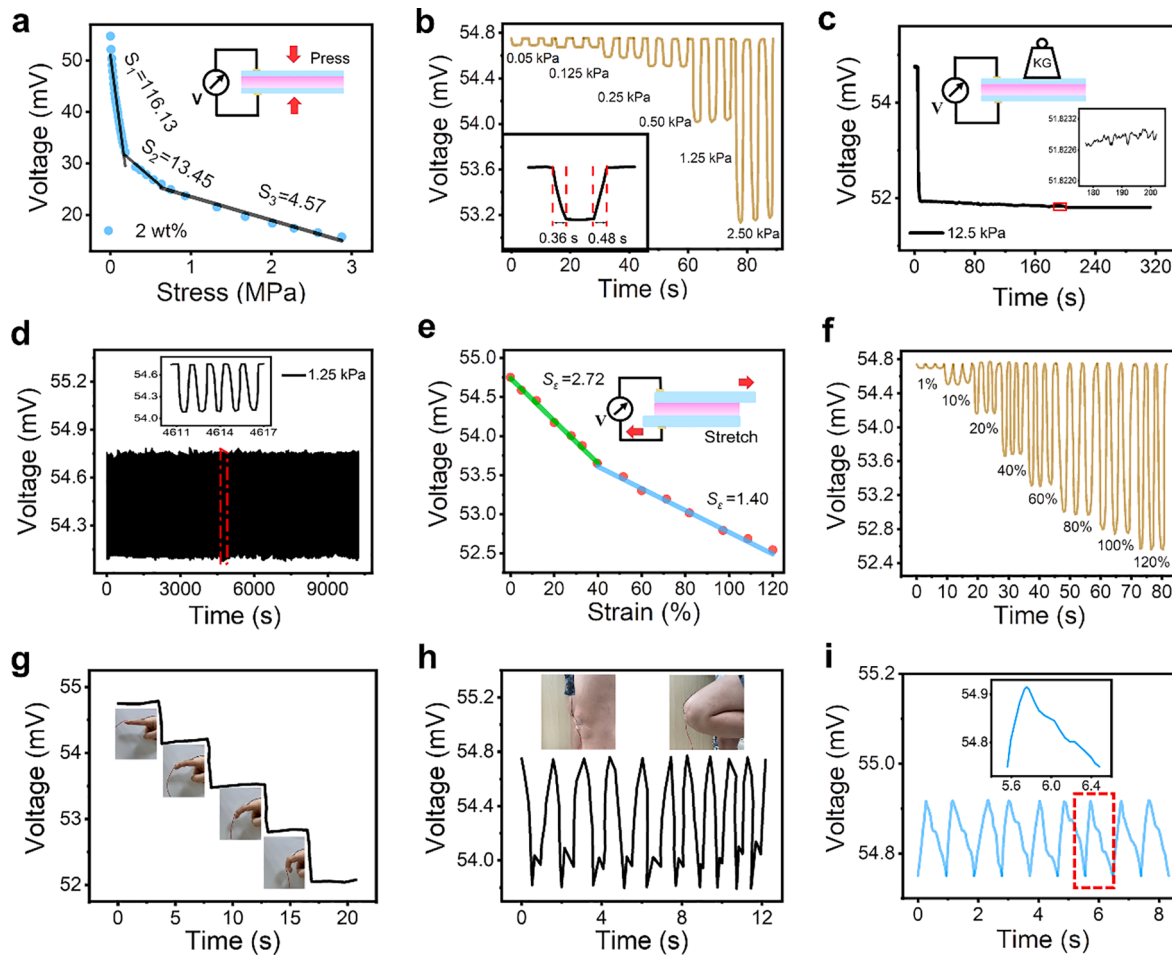


Fig. 3. Pressure- and strain-sensing performance of the receptors. (a) Output voltage of SPI-receptors prepared with a MCS content of 2% as a function of pressure. (b) Pressure sensitivity. (c) Different low-frequency (0.2 Hz) pressures, (d) Repeated loading/unloading of 1.25 kPa pressure for ~10000 cycles, (e) Gradually increased tensile strain, and (f) Different low-frequency (0.3 Hz) tensile strain. Recorded voltage signals of the receptors in response to (g) finger joint motions, (h) knee joint motions and (I) human pulse.

ions (CH_3COO^-) at HD side and LD side of gradient hydrogel, respectively.

The gradient polyelectrolyte hydrogels can be regarded as an aggregate of numerous ultrathin homogeneous layers, and the density of charged groups of these layers increases along the vertical direction (Fig. 4a). According to Equations (1), the potential difference $\Delta\phi(k)$ between the middle of any two adjacent ultrathin layers (k^{th} and $(k+1)^{\text{th}}$ layer) can be represented as:

$$\Delta\phi(k) = \frac{RT}{F} \ln \frac{c_{Ac-(k+1)}}{c_{Ac-(k)}} \quad (2)$$

where $c_{Ac-(k)}$ and $c_{Ac-(k+1)}$ represent the concentrations of CH_3COO^- at the middle of k^{th} layer and $(k+1)^{\text{th}}$ layer. Thus, the total built-in potential of gradient PAM/MCS hydrogels can be transformed into

$$\Delta\phi = \sum_{k=1}^{n-1} \Delta\phi(k) = \frac{RT}{F} \ln \frac{c_{Ac-(n)}}{c_{Ac-(1)}} \quad (3)$$

where $c_{Ac-(n)}$ and $c_{Ac-(1)}$ represent the concentrations of CH_3COO^- at top surface of n^{th} ultrathin layer and the bottom surface of 1th ultrathin layer, respectively.

When the receptors are subjected to a stretching or pressing force, the thickness of each ultrathin layer decreases (Fig. 4a), leading to a decrease of diffusion distance and more CH_3COO^- diffuses from the $(k+1)^{\text{th}}$ layer to k^{th} layer (or from n^{th} layer to 1th layer). Therefore, the ratio of $c_{Ac-(k+1)}/c_{Ac-(k)}$ and $c_{Ac-(n)}/c_{Ac-(1)}$ is decreased, leading to the

decrease of the output voltage of SPI-receptor under stretching or pressing (Equations (2) and (3)). Furthermore, in order to validate above sensing mechanism, we have prepared two kinds of asymmetric hydrogels consisting of two-layer and three-layer homogeneous PAM/MCS hydrogels, respectively. The upper layer has a higher MCS content than the lower layer (Fig. 4b-d). Just as we expected, the output voltage of the asymmetric hydrogels increases with the increasing of the thickness of each PAM/MCS hydrogel layer (Fig. 4b and c), and decreases with the reduction of charge density ratio of upper and lower PAM/MCS layers (Fig. 4d). To further validate the thickness-dependent self-induced potentials of SPI-receptors, we have systematically studied the effect of water content on the pressure sensitivity (Figure S12). As predicted, the SPI-receptors with low water contents displayed the low pressure sensitivity due to the high modulus and hence the increased resistance to compress stress.

3.4. Multiple sensing performance and mechanism

Resembling the functions of human perceptual systems, the receptor can perceive a variety of external stimuli via potential variations. For instance, the output voltage of the receptor increased when its surface of HD side touched to heat source, while a decreased output voltage was observed when the LD side contacted the heat source (Figure S13a). Its temperature sensitivities are ~ 0.20 and $0.19 \text{ mV}/^\circ\text{C}$, as the HD and LD sides touch the heat source, respectively (Fig. 5a). Noteworthily, the receptors can detect the temperature distribution around a heat source

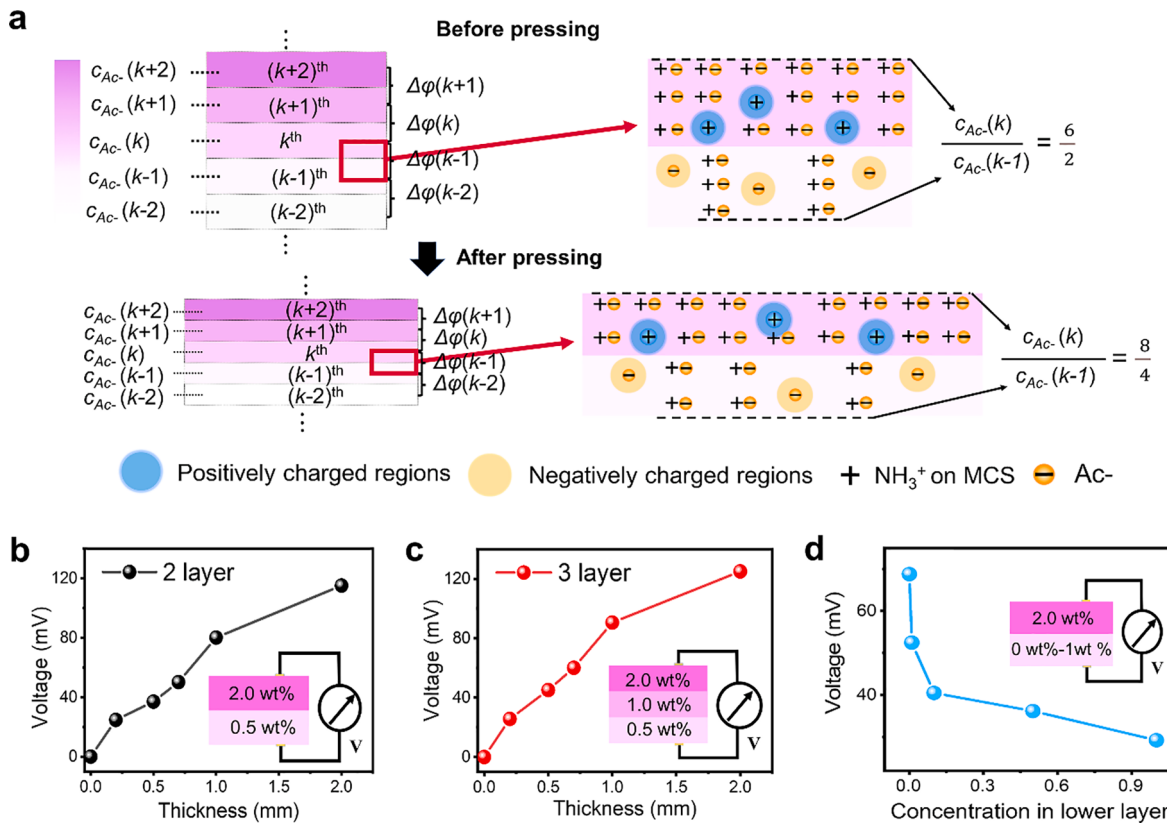


Fig. 4. Mechanoelectric conversion mechanism of gradient polyelectrolyte hydrogels. (a) Schematic illustration of pressure- and stain-sensing mechanism of gradient polyelectrolyte hydrogels. Verification experiments for the above mechanism: thickness-dependent output voltage of asymmetric (b) two-layer and (c) three-layer homogeneous PAM/CS hydrogels with different thickness. The CS contents from the bottom layer to upper layer of two-layer and three-layer PAM/CS hydrogels are 0.5-to-2.0 wt%, and 0.5-to-1.0-to-2.0 wt%, respectively. (d) Output voltage of two-layer PAM/CS hydrogels prepared with different CS concentrations. The MCS concentration of upper layer is fixed at 2.0 wt%, whereas that of bottom layer varies from 0 wt% to 1 wt%.

based on the voltage signal in a non-contact mode (Fig. 5b). When the LD side surface attached to the 0 °C container, the voltage progressively increased with the reduced distance between a receptor and heat source. Vice versa, the voltage continuously decreased with the reduced distance when HD side surface attach to a 0 °C container. Notably, a minimum temperature difference of 0.9 °C along with distance variation can be recognized (Figure S14). The receptor attached onto a finger can also perceive the ambient temperature like human skins in a non-contact mode at a fixed distance of 2 cm (Fig. 5c, and Figure S13b). The output voltage increased when the HD side faced a heat source (≥ 40 °C), while it decreased when the HD side faced a low temperature heat source (≤ 30 °C). A small temperature change of 2.9 °C can be recognized (Figure S13c). This suggests that the real temperature of heat source can be deduced according to the temperature distribution perceived in a non-contact perception mode. It allows for diverse applications such as touchless control and contact warning.

The thermal response stems from the potential variation induced by discrepant diffusion velocity of Na^+ and Cl^- .^[47] For instance, when the HD side of the receptor contacts the heat source, more Cl^- diffuse from HD side to LD side than Na^+ because of the anion-selectivity of gradient PAM/MCS polycation hydrogels (Fig. 5d). Thus, the concentrations of net positive and negative ions inside the two ionic hydrogels increase, giving rise to the increased output voltage of the receptors.^[48] However, the output voltage goes down when the LD side of a receptor contact a heat source, due to the preferential diffusion of Cl^- from LD side to HD side. Besides, we have explored the heat-induced voltage variation of the receptors prepared with the gradient PAM/MSA (methacrylated sodium alginate) hydrogel, which generates a negative output voltage.^[51] As predicted, a heat source approaching or contacting the HD or LD side of the receptor can induce an increase or

decrease of its absolute voltage, respectively, further validating the temperature-sensing mechanism (Figure S15 and S16).

Similarly, the additional saline solution can also trigger ion migration across ionic hydrogels, bringing potential variation and thus can perceive salinity and pH of solutions. Specifically, when a low concentration of NaCl solution (5 μL) is dropped on the surface of PAM/NaCl hydrogel located on HD side, compared with Na^+ , more Cl^- will diffuse from the hydrogel to the additional NaCl solution because of the anion-selectivity of PAM/NaCl polycation hydrogels (Fig. 5d).^[52–54] This leads to the increased net positive ions and hence an increased output voltage of SPI-receptor. A very low concentration of 10^{-5} M for NaCl solution can be detected based on the voltage variation (Fig. 5e). Whereas the addition of high concentration of NaCl solution enable more Cl^- diffuse into PAM/NaCl hydrogels, leading to a decreased net positive ions and a decreased output voltage. Similarly, when the NaCl solution is dropped on the surface of PAM/NaCl hydrogel located at LD side, the opposite potential variation signals can be observed (Fig. 5e and S17a). In addition, after replacing the PAM/NaCl hydrogels of the receptors with PAA/NaCl hydrogels, Na^+ prefers to diffuse under differential concentrations. Thus, the dropping of NaCl solution on the receptor from the same direction bring opposite potential variations (Fig. 5f, and S17b).^[52–54] Besides, we have also explored the voltage variation of receptor prepared with the gradient PAM/MSA hydrogel (Figure S18). Consistent with the theoretical analysis, the output voltage variation of receptor is also mainly determined by their ionic hydrogel electrodes.

Considering the ionization degree or ionic-selectivity of the ionic hydrogel electrodes are highly dependent on pH values, the receptors can also distinguish the additional acid, base and salt solutions. For example, when PAM/NaCl polycation hydrogels were used as ionic

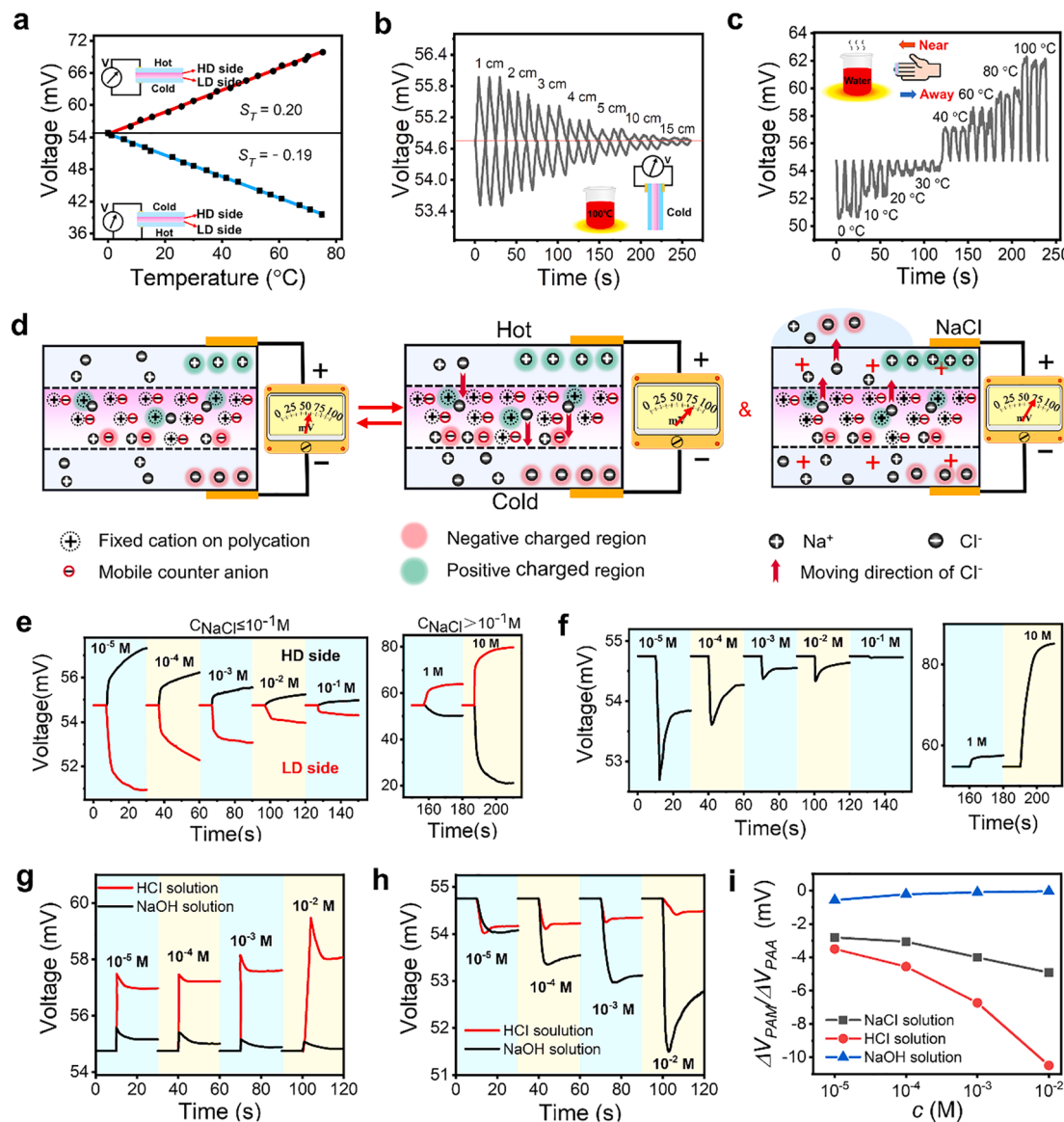


Fig. 5. Temperature, salinity and pH sensing performance and mechanism. (a) Temperature sensitivities of the receptor when the HD side surface and LD side surface contact the heat sources, respectively. (b) Output voltage of the receptor attached to a 0 °C container in response to the distance variation between receptor and 100 °C heat source. (c) Recorded voltage signals of the receptor attached on a finger in response to temperature variation of heat sources, at a fixed distance of 2 cm. (d) Schematic illustration of temperature-sensing and salinity-sensing mechanisms of the SPI-receptor. Recorded voltage signals of the SPI-receptor with PAM/NaCl (e) and PAA/NaCl (f) hydrogels as ionic hydrogels when different concentrations of NaCl solutions (5 μ L) were dropped on the HD and LD sides, respectively. Recorded voltage signals in response to pH variation of the SPI-receptors prepared with the (g) PAM/NaCl and (h) PAA/NaCl hydrogels as ionic hydrogels, respectively. (i) $\Delta V_{PAM}/\Delta V_{PAA}$ in response to the NaCl, HCl, and NaOH solutions with different concentrations.

hydrogel electrodes, the HCl solution can induce a larger amplitude of voltage variation compared to the NaCl solution due to the increased ionization degree (or anion-selectivity) of PAM/NaCl hydrogel (Fig. 5g, and Figure S19a). Accordingly, the NaOH solution induces the smallest amplitude of voltage variation due to the decreased ionization degree. When the PAA/NaCl polyanion hydrogels are used as ionic hydrogel electrodes, the NaOH solution can increase its ionic-selectivity and thus present a larger amplitude of voltage variation (Fig. 5h, and Figure S19b). Therefore, we can evaluate the external solution property according to the value of $\Delta V_{PAM}/\Delta V_{PAA}$, where ΔV_{PAM} and ΔV_{PAA} are the voltage change of the receptors prepared with PAM/NaCl and PAA/NaCl hydrogel electrodes, respectively. The property of the added solution can be inferred according to the inequality: $\Delta V_{PAM}/\Delta V_{PAA}(\text{HCl}) > \Delta V_{PAM}/\Delta V_{PAA}(\text{NaCl}) > \Delta V_{PAM}/\Delta V_{PAA}(\text{NaOH})$ (Fig. 5i). The concentrations of added solutions can be deduced with a high resolution of 10^{-5} M based on the voltage change of the receptors.

An excellent receptor should distinguish the mutual disturbance of the signals of pressure, temperature and salinity. When the SPI-receptors are used as ionic skins, they can distinguish the voltage changes caused by pressure stimulation and thermodiffusion. Under the external pressure, the output voltage of SPI-receptor decreased sharply to a constant value (Fig. 3c), while its output voltage gradually close to the equilibrium value in ~ 10 s upon the trigger of temperature difference (Figure S13a). When exposed to the pressure and thermo stimuli simultaneously, the changed voltage signals of SPI-receptors can thus be divided into two parts, namely the abruptly decreased voltage signals stemming from the pressure (ΔV_P) and gradual changed voltage signals induced by the thermodiffusion (ΔV_T). Figure S20 shows the total voltage change, ΔV_P and ΔV_T of SPI-receptors in response to the combination of pressure and temperature stimuli. Clearly, the SPI-receptors show the analogical ΔV_T at the same temperature under different pressures (Figure S20a, d and h) and similar ΔV_P at the same pressure under

different temperature differences (Figure S20b, e and g). Changing the direction of heat source does not affect the sensing performance (Figure S20c, f and i). Such results demonstrate the feasibility of using SPI-receptors as ionic skins to distinguish the voltage changes caused by pressure stimulation and thermodiffusion. Additionally, when the receptors are used as the ionic tongues, because the dropped NaCl, HCl or NaOH solutions on the surface of SPI-receptors were only 5 μL , the temperature show very little influence on their output voltage SPI-receptor. As shown in Figure S21, the SPI-receptors displayed the similar voltage signals, when the different temperatures of NaCl solutions with same concentrations were dropped on their surfaces.

4. Conclusion

Inspired by diverse receptors in human sensory systems, we have developed a versatile strategy to design fully ionic self-powered receptors for the precise perception of multiple stimuli. The gradient polyelectrolyte hydrogels have been firstly exploited as ion-based mechanoelectric conversion materials, possessing pressure-sensitive self-induced potentials similar to the reported ionic diodes, but circumvent their delamination risk. The self-powered ionic receptor is integrated by sandwiching a gradient polyelectrolyte hydrogel between two stretchable ionic hydrogel electrodes, in which the gradient hydrogel and ionic hydrogels resemble polarized sensory cell membrane and extracellular/intracellular electrolytes, respectively. Thanks to the sandwich structure, the resulting self-powered ionic receptors are transparent, stretchable and multifunctional. They can not only precisely perceive the tiny variation of pressure change based on the thickness-dependent potential of gradient hydrogel, but also accurately detect the temperature, salinity and pH according to the potential variations caused by thermodiffusion and salinity gradient. Different from the ionic-electronic hybrid strategy, such self-powered sensors consisting entirely of ionic conductors could contribute to the development of complex humanlike sensing systems in the future.

Declaration of Competing Interest

The authors declare that they have no known competing financial interests or personal relationships that could have appeared to influence the work reported in this paper

Acknowledgements

This work was supported by the National Natural Science Foundation of China (52003133, 52000110, 51873094 and 51573080), the Natural Science Foundation of Shandong Province (ZR2019QD019), and Program for Taishan Scholar of Shandong Province.

Appendix A. Supplementary data

Supplementary data to this article can be found online at <https://doi.org/10.1016/j.cej.2022.135610>.

References

- [1] I. You, D.G. Mackanic, N. Matsuhisa, J. Kang, J. Kwon, L. Beker, J. Mun, W. Suh, T. Y. Kim, J.-H. Tok, Z. Bao, U. Jeong, Artificial multimodal receptors based on ion relaxation dynamics, *Science* 370 (6519) (2020) 961–965.
- [2] R. Ikeda, M. Cha, J. Ling, Z. Jia, D. Coyle, J. Gu, Merkel cells transduce and encode tactile stimuli to drive $\text{A}\beta$ -afferent impulses, *Cell* 157 (3) (2014) 664–675.
- [3] M.L. Jin, S. Park, Y. Lee, et al., An ultrasensitive, visco-poroelastic artificial mechanotransducer skin inspired by piezo2 protein in mammalian merkel cells, *Adv. Mater.* 29 (2017) 1605973.
- [4] E. Kandel, J. Schwartz, T. Jessell, S. Siegelbaum, A.J. Hudspeth, Principles of Neural Science (New York, 2000).
- [5] R. Matsuo, Role of saliva in the maintenance of taste sensitivity, *Crit. Rev. Oral Biol. Med.* 11 (2) (2000) 216–229.
- [6] J. Yeom, A. Choe, S. Lim, Y. Lee, S. Na, H. Ko, Soft and ion-conducting hydrogel artificial tongue for astringency perception, *Sci. Adv.* 6 (2020) eaaba5785.
- [7] Y. Chang, L. Wang, R. Li, Z. Zhang, Q. Wang, J. Yang, C.F. Guo, T. Pan, First decade of interfacial ionic sensing: from droplet sensors to artificial skins, *Adv. Mater.* 33 (2021) 2003464.
- [8] N. Bai, L. Wang, Q. Wang, et al., Graded intrafillable architecture-based iontronic pressure sensor with ultra-broad-range high sensitivity, *Nat. Commun.* 11 (2020) 209.
- [9] Z. Wang, S. Guo, H. Li, et al., The semiconductor/conductor interface piezoresistive effect in an organic transistor for highly sensitive pressure sensors, *Adv. Mater.* 31 (2018) 1805630.
- [10] X. Wu, M. Ahmed, Y. Khan, M.E. Payne, J. Zhu, C. Lu, J.W. Evans, A.C. Arias, A potentiometric mechanotransduction mechanism for novel electronic skins, *Sci. Adv.* 6 (30) (2020).
- [11] D. Zhang, H. Qiao, W. Fan, K. Zhang, Y. Xia, K. Sui, Self-powered ionic sensors overcoming the limitation of ionic conductors as wearable sensing devices, *Mater. Today Phys.* 15 (2020), 100246.
- [12] Y. Zang, F. Zhang, D. Huang, X. Gao, C.-A. Di, D. Zhu, Flexible suspended gate organic thin-film transistors for ultra-sensitive pressure detection, *Nat. Commun.* 6 (2015) 6269.
- [13] C. Li, S. Yang, Y. Guo, et al., Flexible, multi-functional sensor based on all-carbon sensing medium with low coupling for ultrahigh-performance strain, temperature and humidity sensing, *Chem. Eng. J.* 425 (2021), 131523.
- [14] Z. Lei, P. Wu, A highly transparent and ultra-stretchable conductor with stable conductivity during large deformation, *Nat. Commun.* 10 (2019) 3429.
- [15] C. Li, S. Yang, Y. Guo, et al., Flexible, multi-functional sensor based on all-carbon sensing medium with low coupling for ultrahigh-performance strain, temperature and humidity sensing, *Chem. Eng. J.* 426 (2021), 130364.
- [16] K.-Y. Chun, Y.J. Son, E.-S. Jeon, S. Lee, C.-S. Han, A self-powered sensor mimicking slow- and fast-adapting cutaneous mechanoreceptors, *Adv. Mater.* 30 (2018) 1706299.
- [17] C. Zhang, B. Wu, Y. Zhou, F. Zhou, W. Liu, Z. Wang, Mussel-inspired hydrogels: from design principles to promising applications, *Chem. Soc. Rev.* 49 (2020) 3605–3637.
- [18] Z. Yu, P. Wu, Underwater communication and optical camouflage ionogels, *Adv. Mater.* 33 (2021) 2008479.
- [19] G. Gao, F. Yang, F. Zhou, et al., Bioinspired self-healing human-machine interactive touch pad with pressure-sensitive adhesiveness on targeted substrates, *Adv. Mater.* 32 (2020) 2004290.
- [20] S. Li, N. Pan, Z. Zhu, R. Li, B. Li, J. Chu, G. Li, Y.u. Chang, T. Pan, All-in-one iontronic sensing paper, *Adv. Funct. Mater.* 29 (11) (2019) 1807343.
- [21] Y. Wang, X. Cao, J. Cheng, B. Yao, Y. Zhao, S. Wu, B. Ju, S. Zhang, X. He, W. Niu, cephalopod-inspired chromotropic ionic skin with rapid visual sensing capabilities to multiple stimuli, *ACS Nano* 15 (2) (2021) 3509–3521.
- [22] Y. Zhou, Y. Hou, Q. Li, et al., Biocompatible and flexible hydrogel diode-based mechanical energy harvesting, *Adv. Mater. Technol.* 2 (2017) 1700118.
- [23] N. Gogurla, B. Roy, S. Kim, Self-powered artificial skin made of engineered silk protein hydrogel, *Nano Energy* 77 (2020), 105242.
- [24] Y. Zhou, C. Wan, Y. Yang, et al., Highly stretchable, elastic, and ionic conductive hydrogel for artificial soft electronics, *Adv. Funct. Mater.* 29 (2019) 1806220.
- [25] H.-R. Lee, J. Woo, S.H. Han, et al., A stretchable ionic diode from copolyelectrolyte hydrogels with methacrylated polysaccharides, *Adv. Funct. Mater.* 29 (2019) 1806909.
- [26] K. Dong, Z. Wu, J. Deng, et al., A stretchable yarn embedded triboelectric nanogenerator as electronic skin for biomechanical energy harvesting and multifunctional pressure sensing, *Adv. Mater.* 30 (2018) 1804944.
- [27] P. Zhang, Y. Chen, Z.H. Guo, W. Guo, X. Pu, Z.L. Wang, Stretchable, transparent, and thermally stable triboelectric nanogenerators based on solvent-free ion-conducting elastomer electrodes, *Adv. Funct. Mater.* 30 (2020) 1909252.
- [28] T. Liu, M. Liu, S.u. Dou, J. Sun, Z. Cong, C. Jiang, C. Du, X. Pu, W. Hu, Z.L. Wang, Triboelectric-nanogenerator-based soft energy-harvesting skin enabled by toughly bonded elastomer/hydrogel hybrids, *ACS Nano* 12 (3) (2018) 2818–2826.
- [29] X. Pu, H. Guo, J. Chen, X. Wang, Y.i. Xi, C. Hu, Z.L. Wang, Zhong Lin Wang, Eye motion triggered self-powered mechanosensational communication system using triboelectric nanogenerator, *Sci. Adv.* 3 (7) (2017), e1700694.
- [30] K. Meng, J. Chen, X. Li, et al., Flexible weaving constructed self-powered pressure sensor enabling continuous diagnosis of cardiovascular disease and measurement of cuffless blood pressure, *Adv. Funct. Mater.* 29 (2019) 1806388.
- [31] D. Zhang, W. Yang, W. Gong, et al., Abrasion resistant/waterproof stretchable triboelectric yarns based on fermat spirals, *Adv. Mater.* 33 (2021) 2100782.
- [32] S. Zhang, Y. Wang, X. Yao, P.L. Floch, X. Yang, J. Liu, Z. Suo, Stretchable electrets: nanoparticle-elastomer composites, *Nano Lett.* 20 (2020) 4580–4587.
- [33] R. Fu, L. Tu, Y. Zhou, L. Fan, F. Zhang, Z. Wang, J. Xing, D. Chen, C. Deng, G. Tan, P. Yu, L. Zhou, C. Ning, A tough and self-powered hydrogel for artificial skin, *Chem. Mater.* 31 (23) (2019) 9850–9860.
- [34] R. Fu, L. Tu, Y. Zhou, et al., An all-organic elastomeric electret composite, *Adv. Mater.* 29 (2017) 1603813.
- [35] A. Kachroudi, S. Basrour, L. Rufer, A. Sylvestre, F. Jomni, Micro-structured PDMS piezoelectric enhancement through charging conditions, *Smart Mater. Struct.* 25 (2016), 105027.
- [36] X. Wang, W.-Z. Song, M.-H. You, J. Zhang, M. Yu, Z. Fan, S. Ramakrishna, Y.-Z. Long, Bionic single-electrode electronic skin unit based on piezoelectric nanogenerator, *ACS Nano* 12 (8) (2018) 8588–8596.
- [37] H.J. Kim, B. Chen, Z. Suo, R.C. Hayward, Ionoelastomer junctions between polymer networks of fixed anions and cations, *Science* 367 (6479) (2020) 773–776.
- [38] Y. Zhang, C.K. Jeong, J. Wang, et al., Hydrogel ionic diodes toward harvesting ultralow-frequency mechanical energy, *Adv. Mater.* 36 (2021) 2103056.

- [39] Y. Hou, Y. Zhou, L. Yang, et al., Flexible ionic diodes for low-frequency mechanical energy harvesting, *Adv. Energy Mater.* 7 (2017) 1601983.
- [40] B. Ying, Q. Wu, J. Li, X. Liu, An ambient-stable and stretchable ionic skin with multimodal sensation, *Mater. Horiz.* 7 (2) (2020) 477–488.
- [41] M.C.G. Pellá, A.R. Simão, M.K. Lima-Tenório, E. Tenório-Neto, D.B. Scariot, C.V. Nakamura, A.F. Rubira, Chitosan hybrid microgels for oral drug delivery, *Carbohydr. Polym.* 239 (2020), 116236.
- [42] B.J.P. Gong, Y. Katsuyama, T. Kurokawa, Y. Osada, Double-network hydrogels with extremely high mechanical strength, *Adv. Mater.* 15 (2003) 1155–1158.
- [43] H. Wang, Y. Sun, T. He, et al., Bilayer of polyelectrolyte films for spontaneous power generation in air up to an integrated 1,000 V output, *Nat. Nanotechnol.* 16 (2021) 811.
- [44] Y. Huang, H. Cheng, C. Yang, et al., Interface-mediated hygroelectric generator with an output voltage approaching 1.5 volts, *Nat. Commun.* 9 (2018) 4166.
- [45] Z. Sun, L. Feng, X. Wen, L. Wang, X. Qin, J. Yu, Nanofiber fabric based ion-gradient-enhanced moist-electric generator with a sustained voltage output of 1.1 volts, *Mater. Horiz.* 8 (8) (2021) 2303–2309.
- [46] Y. Zhang, C.K. Jeong, J.J. Wang, X. Chen, K.H. Choi, L.-Q. Chen, W. Chen, Q. M. Zhang, Q. Wang, Hydrogel ionic diodes toward harvesting ultralow-frequency mechanical energy, *Adv. Mater.* 33 (2021) 2103056.
- [47] F.F. Gao, Z. Zhang, X. Zhao, L.L. An, L.X. Xu, X.C. Xun, B. Zhao, T. Ouyang, Z. Kang, Q.L. Liao, Yue Zhang, Highly conductive and stretching-insensitive films for wearable accurate pressure perception, *Chem. Eng. J.* 429 (2022) 132488.
- [48] Q. Su, Q. Zou, Y. Li, Y.Z. Chen, S.Y. Teng, J.T. Kelleher, R. Nith, P. Cheng, N. Li, W. Liu, S.L. Dai, Y.D. Liu, A. Mazursky, J. Xu, L.H. Jin, P. Lopes, S.H. Wang, A stretchable and strain-unperturbed pressure sensor for motion interference-free tactile monitoring on skins, *Sci. Adv.* 7 (2021) eabi4563.
- [49] Y. Wang, S. Gong, S.J. Wang, G.P. Simon, W. Cheng, Volume-invariant ionic liquid microbands as highly durable wearable biomedical sensors, *Mater. Horiz.* 3 (3) (2016) 208–213.
- [50] C.-G. Han, X. Qian, Q. Li, B. Deng, Y. Zhu, Z. Han, W. Zhang, W. Wang, S.-P. Feng, G. Chen, W. Liu, Giant thermopower of ionic gelatin near room temperature, *Science* 368 (6495) (2020) 1091–1098.
- [51] F. Araiza-Verduzco, E. Rodríguez-Velázquez, H. Cruz, I.A. Rivero, D.R. Acosta-Martínez, G. Pina-Luis, M. Alatorre-Meda, Photocrosslinked alginate-methacrylate hydrogels with modulable mechanical properties: effect of the molecular conformation and electron density of the methacrylate reactive group, *Materials* 13 (2020) 534.
- [52] Z. Zhang, L. He, C. Zhu, Y. Qian, L. Wen, L. Jiang, Improved osmotic energy conversion in heterogeneous membrane boosted by three-dimensional hydrogel interface, *Nat. Commun.* 11 (2020) 875.
- [53] X. Zhu, J. Hao, B. Bao, Y. Zhou, H. Zhang, J. Pang, Z. Jiang, L. Jiang, Unique ion rectification in hypersaline environment: a high-performance and sustainable power generator system, *Sci. Adv.* 4 (10) (2018).
- [54] Z. Zhang, S. Yang, P. Zhang, J. Zhang, G. Chen, X. Feng, Mechanically strong mxene/kevlar nanofiber composite membranes as high-performance nanofluidic osmotic power generators, *Nat. Commun.* 10 (2019) 2920.